I&EC research
Industrial & Engineering Chemistry Research

Research Note

pubs.acs.org/IECR

A Functional Full-Scale Heat Exchanger Coated with Aluminum Fumarate Metal–Organic Framework for Adsorption Heat Transformation

Harry Kummer,[†,‡] Felix Jeremias,[†] Alexander Warlo,[†] Gerrit Füldner,[†] Dominik Fröhlich,[†,∥] Christoph Janiak,[∥] Roger Gläser,[‡] and Stefan K. Henninger*[,†]

[†]Division Thermal Systems and Buildings, Fraunhofer Institute for Solar Energy Systems ISE, Heidenhofstraße 2, 79110 Freiburg, Germany

[∥]Institut für Anorganische Chemie und Strukturchemie, Universität Düsseldorf, 40204 Düsseldorf, Germany

[‡]Institut für Technische Chemie, Universität Leipzig, Linnéstraße 3, 04103 Leipzig, Germany

Supporting Information

ABSTRACT: Metal–organic frameworks represent a class of microporous adsorbents with high application potential for adsorption heat transformation. Here, we present a functional, full-scale heat exchanger coated with the microporous aluminum fumarate MOF Basolite A520 using a polysiloxane-based binding agent. The function of the heat exchanger was evaluated resulting in a gross cooling power of 2900 W (at the beginning of the adsorption cycle) or, respectively an average cooling power of 690 W (up to a limit of 90% equilibrium loading in 7 min) under the working conditions of a realistic adsorption chiller of 90 °C – 30 °C – 18 °C (temperature level of heat source, heat rejection/condenser, and evaporator).

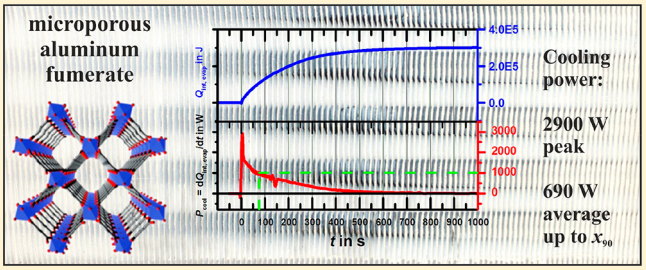

INTRODUCTION

Metal–organic frameworks (MOFs) receive continuous attention as microporous adsorbents due to their unsurpassed porosity and chemical variability. MOFs provide an enormous potential for improvement in several fields of application, such as gas storage,[1−8] gas[9−13] and liquid[14−17] separation, heterogeneous catalysis,[18−22] drug delivery,[23,24] or sensor applications.[25−27] On the basis of their favorable water vapor adsorptive properties,[28−30] they are especially attractive for sorption-based heat transformation.[31−42] Among the different MOFs used for this purpose, microporous aluminum fumarate[43] has proven especially promising because of its comparatively high hydrophilicity and excellent multicycle stability[34] (virtually no loss for 4500 ad-/desorption cycles using advantageous water as the working fluid). Moreover, aluminum fumarate is accessible by a cost-efficient synthesis, which can be achieved by precipitation from low-cost bulk chemicals in water at ambient pressure.[44]

Thermally driven adsorption heat pumps (AHPs) can be applied to gain more heating energy from a given amount of fuel than from its mere combustion enthalpy. Thermally driven chillers (TDCs), on the other hand, make use of waste heat (such as heat from combined power and heat cycles, or district heat, during the hot season) for the production of useful cold. The underlying process has been discussed in detail in the literature.[34,36,45−47] However, for the realization of an efficient adsorption heat pump or chiller, the adsorbent has to meet several requirements. Most importantly, the adsorbent must be thermally coupled to the fluid circuit as efficiently as possible, as the adsorption kinetics and hence the power and power density of the unit directly depend on the transfer of heat of adsorption away from and toward the adsorption site.[48−50] Therefore, heat exchangers coated with the adsorbent (HX, in the following referred to as *adsorbers*) are by far superior to packed beds in terms of power delivered per mass of adsorbent.[51−56] Due to the cyclic nature of the process, the overall mass of the adsorber in relation to the adsorption capacity, must be kept as low as possible in order to minimize losses by heating and cooling passive thermal mass. Maximizing the amount of adsorbent coating on a HX and, in addition, achieving fast and efficient heat and mass transfer through the adsorbent, are among the major challenges for the design of adsorbent-coated heat exchangers. Furthermore, the coating has to be mechanically and chemically stable toward thermal stress, due to the cyclic operation, mechanical shocks, and vibration, for example, due to transportation. These issues are addressed in the literature by the development and evaluation of several routes to obtain thick and sturdy binder-based or binder-free coatings, not only for conventional adsorbents, but also for promising MOFs such

Received: January 9, 2017
Revised: June 6, 2017
Accepted: July 10, 2017
Published: July 10, 2017

DOI: 10.1021/acs.iecr.7b00106
Ind. Eng. Chem. Res. 2017, 56, 8393−8398

as CAU-10-H, HKUST-1 or MIL-101(Cr).[34,50,51,57−62] Yet the scale-up toward a functional, fully coated MOF-based HX has not yet been reported so far. This may be attributed to the fact that the procurement, formulation, and deposition of the large amounts of suitable MOFs needed for such applications is arduous on a scale larger than in the laboratory.

In this contribution, we present the fabrication of a functional full-scale HX coated with aluminum fumarate MOF using a polysiloxane binder. Moreover a benchmark evaluation of the HX with respect to adsorption equilibrium and kinetics as well as cooling performance was conducted.

EXPERIMENTAL PROCEDURE

Procurement. A state-of-the-art water/air finned HX with aluminum fins pressed onto copper tubes (diameter of copper tubes = 12 mm, aluminum fins with thickness = 0.2 mm, fin spacing = 3.0 mm, total dimensions of 480 × 160 × 120 mm^3, overall volume filled with lamellas = 385 × 160 × 110 mm^3 = 6776 L, total mass of 3001 g) was manufactured by WÄTAS Wärmetauscher Sachsen GmbH, Olbernhau, Germany (see Figure 1a). Microporous aluminum fumarate (Basolite A520, BET surface of 970 m^2/g) was supplied by BASF SE.[44] The polysiloxane binder emulsion (SilRes MP50 E) was obtained from Wacker Chemie AG.

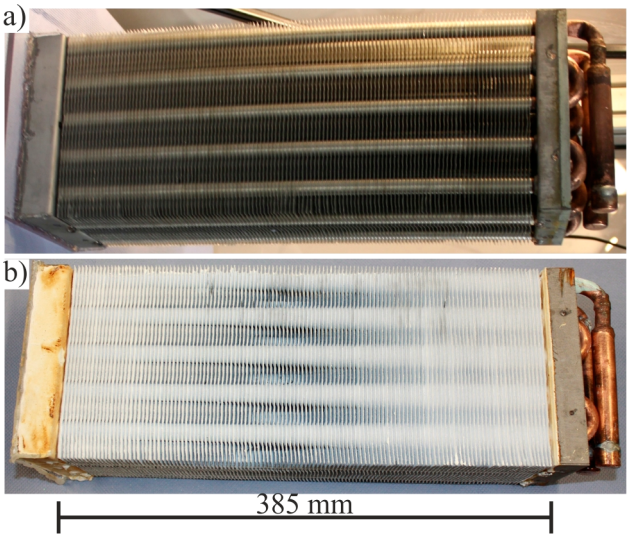

Figure 1. (a) Heat-exchanger (HX) after cleaning and (b) after coating with the aluminum fumarate MOF and drying.

Pretreatment. Prior to application of the coating, the HX was degreased by submersion into a mild alkaline cleaning solution (7 wt % SurTec 140, 0.5 wt % SurTec 089 obtained from SurTec International GmbH) at 80 °C for 5 min, then thoroughly rinsed with deionized water, oxidized by submersion into 13 wt % nitric acid (ACS grade, 69%, Sigma-Aldrich), at RT for 2 min and again rinsed with deionized water, then dried at room temperature with compressed air. The cleaned HX is shown in Figure 1a. Areas not to be coated were covered using adhesive tape.

Preparation of the Coating Dispersion. In a 25 L stainless steel vat (530·330·200 mm^3), 4338 g of microporous aluminum fumarate (5.2 wt % adsorbed water; dry mass content 4121 g) was dispersed in 13.0 L of deionized (DI) water at room temperature using two two-bladed propeller stirrers at 500 rpm for 30 min. The dispersion process was assisted by ultrasonic treatment (Elmasonic x-tra basic 800 at 45 kHz and 1000 W) for 30 min, followed by another 45 min of stirring; 2594 g of polysiloxane binder (dry mass content 1258 g) was added and stirring was continued for 60 min.

Coating process. The HX was immersed into the freshly prepared dispersion (cf. above) and withdrawn. Excess slurry between lamella was removed by compressed air. The lamellas were put horizontally and dried in air for 60 min, then reimmersed into the dispersion, again withdrawn, excess slurry removed by compressed air and left in air for 6 d at room temperature. After taking off the adhesive tape, removal of volatile contents of the binding agent was assured by heating the coated HX at 200 °C for 3.5 h in an air ventilated furnace.

Immediately after heating, the dry mass of the coated HX was measured. The mass of the applied coating was determined by subtracting the mass of the cleaned HX before coating from the mass of the hot, dried HX. The adsorbent mass fraction of the dispersion w_{Ads} = 0.77, calculated as dry adsorbent mass divided by solid mass of adsorbent and binder in the dispersion. The coating thickness was measured with a digital caliper on eight different spots of the fins, coated on both sides. The fin thickness was subtracted and the thickness of the upper and lower coating was averaged.

Determination of Equilibrium Adsorption Properties. Water vapor adsorption properties were measured isothermally at 25 °C in a Quantachrome VStar up to a p/p_0 = 0.99, after activating the sample at 150 °C for 12 h. To crosscheck adsorption properties of the coating, approximately 1 g of the coating was scraped off the HX lamellas, slightly ground, and measured in the same way as the original powder.

Estimation of Coefficient of Performance (COP) under Cooling Conditions. The cooling COP is defined as useful cooling energy output divided by the required regeneration energy input.

$$\mathrm{COP}_{\mathrm{cool}} = \frac{Q_{\mathrm{evap}}}{Q_{\mathrm{regen}}}$$

The useful cooling energy is simply the enthalpy achieved in the evaporator Q_{evap} and can be calculated as evaporation enthalpy times the total water uptake. The required regeneration energy consists of a sensible part (for heating up the device) and the desorption enthalpy times the total water uptake. The water uptake was interpolated between the measured data sets as Gaussian approximation of three isotherms (25 °C, 40 °C, and 60 °C). For the sensible part, the mass of the height exchanger (3001 g with a specific heat capacity of 900 J kg^{-1} K^{-1}) and binder (150 g with a specific heat capacity of 1200 J kg^{-1} K^{-1}) has been taken into account, whereas the realized adsorbent mass with 493 g was used along with a corresponding heat capacity of 1200 J kg^{-1} K^{-1}. Then the COP was calculated for a set of temperatures as follows: The evaporator temperature was varied from 10 to 22 °C in steps of 2 K, adsorption temperature was fixed at 35 °C, and desorption temperature was 65 °C, as aimed for data center cooling. The heat rejection and adsorption temperature were taken as identical. The uptake was calculated as loading difference between loading at desorption condition x_{des} and loading at adsorption condition x_{ads}.

Dynamic of Adsorption and Cooling Performance Testing. The adsorption and cooling performance of the coated HX was tested in a custom-made apparatus as described in a previous work.[50] The HX was placed into a vacuum sample

DOI: 10.1021/acs.iecr.7b00106
Ind. Eng. Chem. Res. 2017, 56, 8393−8398

chamber, attached to a digital suspension balance and connected to a fluid circuit in such a way that the weight signal was not affected by the tubing. The weight signal was recorded continuously. A sufficiently large evaporator chamber provided a constant, settable water vapor pressure via a solenoid valve. Prior to the adsorption experiment, the adsorber was degassed at a temperature of 90 °C under vacuum (>0.01 kPa) for 12 h and then preloaded at 0.3 kPa for simulating the preloaded state under field operating conditions (desorbing against a condenser at 30 °C). Adsorption was initiated by opening the connection between the sample chamber and the evaporator chamber. Adsorption kinetics and cooling performance were determined at a HX fluid temperature of 30 °C and a constant water vapor pressure of 1.8 kPa, corresponding to an evaporator temperature (useful cold) of 18 °C.

Cooling Performance of the HX. The cooling performance was calculated from the adsorption kinetic experiments as follows: Under isobaric conditions and constant adsorption temperature, it can be anticipated that the evaporated amount of water equals the adsorbed amount of water at any point of time t. Thus, the integral heat of evaporation $Q_{int,evap}(t)$ that has been provided at any time t can be calculated from the adsorbed amount of water $m_{Ads}(t)$ and the standard evaporation enthalpy of water, ΔH^0_{evap} (H_2O) = 2230 kJ/kg according to

$$Q_{int,evap} = m_{Ads}(t)\cdot\Delta H^{\circ}_{evap}(H_2O)$$

The gross cooling power P_{cool}, provided during adsorption by evaporation, is proportional to the evaporation rate, that is, also to the adsorption rate, assuming stationary conditions, and equals the time derivative of the integral heat of evaporation:

$$P_{Cool} = \frac{d}{dt}Q_{int,evap}$$

RESULTS AND DISCUSSION

After final drying of the coated HX, a smooth, homogeneous MOF-binder surface was obtained (see Figure 1b). The final dry weight of the MOF-coated HX was determined at 3644 g, resulting in 643 g of dried coating being applied and therefore 493 g of aluminum fumarate are coated on the HX. This corresponded to a low adsorbent to sensible mass ratio of 0.135 for the overall adsorber. Assuming an even distribution of the dispersion components, the adsorbent mass fraction of the coating can be taken as identical to the w_{ads} of the dispersion, therefore the MOF-adsorbent content of the coating is 77 wt %, corresponding to 23 wt % binder in the coating.

The average thickness of the MOF-containing coating was found to be between 300 and 330 μm, distributed evenly on the aluminum lamellas and copper tubes of the HX. Blocking of the space between the lamellae was not observed. The coating proved mechanically resistant against handling (touchable without flaking) and under conditions of operating during performance testing. After 4 days in the climate chamber and 3 days in the closed dynamic setup, the steel plates at the ends of the HX started to corrode by forming brown rust, probably triggered through removing the zinc galvanized protection layer during treatment in HNO_3 solution. Also the coating on these steel parts had an orange to brown color, probably caused by diffusion of iron oxide into the coating (see Figure 1b, coated steel part on the left end).

A comparison of the equilibrium adsorption isotherms of the coated HX with those of the pure microporous aluminum fumarate (Figure 2) shows that the water loading characteristic of the MOF has largely been maintained. The original, spray-coated material shows an additional rise, starting at a p/p_0 of 0.6. This is probably induced by early condensation through macrostructures of the spray-coated particles which results in high hysteresis of the desorption path. At a p/p_0 = 0.48 (adsorption point at 30 °C against evaporator at 18 °C) the equilibrium loading is x = 0.317 g g^{-1}. The corrected adsorption loading for the adsorbent in the coating is x = 0.309 g g^{-1}, therefore 97% of the adsorption capacity remained. Also comparing with the equilibrium point out of the kinetic measurement at 30 °C and a p/p_0 = 0.48, the loading x is 0.275 g g^{-1}, which corresponds to 88% of the original uptake. Taking into account a lower equilibrium loading at higher temperature (25 to 30 °C), this is consistent with the isothermal measurements. In addition the hydrothermal stability was tested and the capacity of the coating remained at 95% after 360 cycles (see Supporting Information for more details).

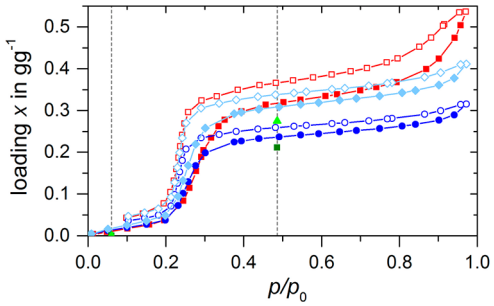

Figure 2. Equilibrium isotherms at 25 °C of the aluminum fumarate powder (red ■), coating (blue ●) and aluminum fumarate (calculated from coating by subtraction of the masses of the binding agent [aqua ◆]) in comparison with the 30 °C equilibrium points of the kinetic setup (coating [dark green ■] and corrected aluminum fumarate [light green ▲]). Adsorption is shown with filled symbols. Gray dotted line shows the operational window of the dynamic measurement.

From published equilibrium data,[34] an estimation of the achievable COP is possible, taking into account the sensible mass of the HX structure and binder without heat recovery. At operating conditions of 90 °C − 30 °C − 18 °C, the equilibrium COP could reach 0.61, and this holds true for realistic cycle loadings of 90%.

The strength of this material is operating conditions with low desorption temperatures not more than 65 °C, for example, data center cooling. The COP overview for a variation of the evaporator temperature at 65 °C heat source and 35 °C heat rejection temperature is shown in Figure 3. It reveals a maximum COP of 0.72 at an evaporator temperature of 22 °C. For data center cooling, with heat rejection at 35 °C and useful cold at 18 °C, the equilibrium cooling COP is 0.69. A wider variation of the COP for heat source temperatures of 65, 70, and 90 °C can be found in the Supporting Information.

The kinetics of the mass gain during water sorption at a constant water vapor pressure of 1.8 kPa with a heat rejection temperature of 30 °C is depicted in Figure 4. The equilibrium loading of 0.275 g g^{-1} was determined at t_{end} = 25 min after starting the experiment. After t_{60} = 3 min the adsorber is already loaded to about 60%, after t_{90} = 7 min it is loaded to 90%, and after 12.5 min, the adsorber is virtually saturated. According to Dawoud[52] the rise-up time $t_{80}-t_{15}$ was calculated to t_r = 270 s, the sorption speed $v_s = (x_{50} - x_0)/t_{50}$ = 0.08 g/100 g

DOI: 10.1021/acs.iecr.7b00106
Ind. Eng. Chem. Res. 2017, 56, 8393−8398

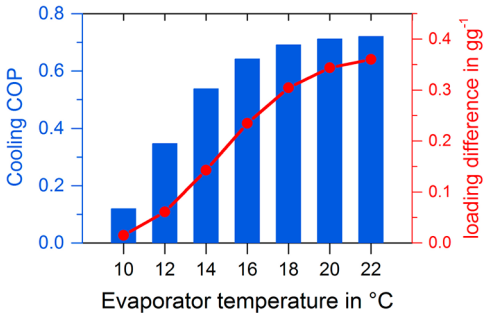

Figure 3. COP calculation for a fixed heat source and heat rejection temperature of 65−35 °C. Blue bars indicate the achievable equilibrium cooling COP of the coated HX without heat recovery, the red dots indicate the calculated loading difference at these operation conditions.

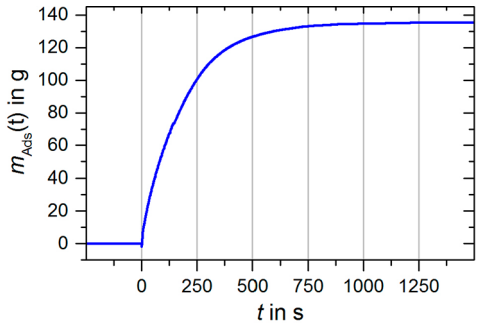

Figure 4. Time dependence of the HX mass gain during adsorption for operating condition 90 °C − 30 °C − 18 °C (blue line). Adsorption started with the valve opening at t = 0 s.

adsorbent/s. Adsorption kinetics for a comparable full scale fin heat exchanger coated with the silicoaluminophosphate SAPO-34 (AQSOA-Z02 by Mitsubishi Chemicals) with a thickness of 300 μm was reported previously by Dawoud et al.[52] In this study, using operating conditions of 90 °C − 35 °C − 5 °C, 57% of the loading was reached after 10 min. Even when taking into consideration the harsher operating condition at lower adsorption pressure of the SAPO-34-coated HX, the water sorption kinetics for the HX coated with the aluminum fumarate MOF clearly shows the huge potential for this application.

According to the mass gain over time (Figure 4), the calculated integral heat of evaporation and the cooling power are provided in Figure 5. A maximum performance of 2900 W is achieved at the beginning of the working cycle. Even at t = 74 s, the cooling power is still in the range of 1000 W. The average cooling power until reaching a loading of 90% is still at 690 W. Dividing P_{Cool} by the volume of the finned part, the volume specific cooling power (VSCP) of the HX can be calculated. A peak VSCP of $VSCP_{peak}$ = 430 W L^{-1} can be achieved, and also with a realistic cycle loading of 90%, the $VSCP_{x90}$ amounts to 101 W L^{-1}. The achieved specific cooling power (SCP) per kilogram of MOF is a crucial value for estimating the cost of the adsorber. SCP calculated for the peak performance is SCP_{peak} = 5880 W kg^{-1} and for x_{90} is SCP_{x90} = 1394 W kg^{-1}. These results show the high potential of this aluminum fumarate-coated HX. From the fast adsorption kinetics, it can be deduced that the MOF particles, which are not excluded from adsorption by blocking through the binding agent, are accessible for unhindered and rapid mass transfer. Furthermore,

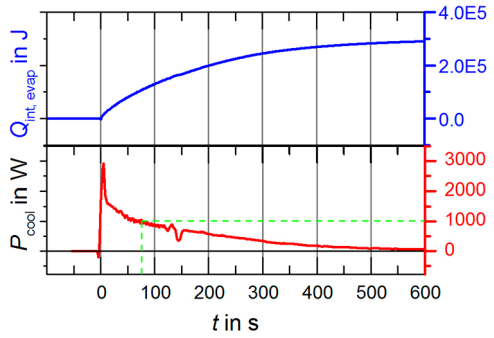

Figure 5. Gross cooling power P_{cool} of the aluminum fumarate-coated HX for operating conditions 90 °C − 30 °C − 18 °C (red line, lower part), calculated from the integral heat of evaporation $Q_{int,evap}$ (blue line, upper part). The derivative was calculated using OriginPro and smoothed with the method of Savitzky−Golay using a 2nd order polynome. The green line indicates P_{Cool} = 1000 W for a half cycle time of t = 74 s.

the steep adsorption isotherm of microporous aluminum fumarate probably also contributes to the fast adsorption and high cooling power, given that pore filling occurs over a small p/p_0 range and the driving force for filling the pores remains high as long as unfilled pores are still present.

SUMMARY AND OUTLOOK

This work shows that a functional heat exchanger fully coated by the MOF aluminum fumarate can be prepared using a convenient binder-based approach. The coating is evenly distributed among the aluminum fins of the HX and is mechanically stable. The equilibrium adsorption properties of the coating are comparable to those of the pure MOF adsorbent. Adsorption kinetics is very fast compared to conventional adsorbers, and the resulting cooling performance (2900 W at the beginning, 690 W average, until 90% loading) is suitable from an industrial point of view. Together with the inherent multicycle stability of microporous aluminum fumarate and the excellent long-term stability of polysiloxane coatings reported in the literature, these results clearly suggest that the technology has the potential for industrial application and can significantly advance sorption-based chilling. Further research should focus on a deeper understanding of the dynamic and COP in comparison to state of the art HX and implementation of the coating process in a technical manufacturing line, corrosion issues, and implementation of other MOFs for different boundary conditions, such as CAU-10-H or MIL-100.

ASSOCIATED CONTENT

Supporting Information

The Supporting Information is available free of charge on the ACS Publications website at DOI: 10.1021/acs.iecr.7b00106.

Long-term cycle stability of aluminum fumarate, COP calculation for heat source temperatures of 65, 70, and 90 °C, and varying heat rejection and evaporator temperatures (PDF)

AUTHOR INFORMATION

Corresponding Author

*E-mail: stefan.henninger@ise.fraunhofer.de.

DOI: 10.1021/acs.iecr.7b00106
Ind. Eng. Chem. Res. 2017, 56, 8393−8398

ORCID
Harry Kummer: 0000-0002-2269-5996
Christoph Janiak: 0000-0002-6288-9605

Notes
The authors declare no competing financial interest.

■ ACKNOWLEDGMENTS

Funding by the Fraunhofer Society under Grant No. MAVO 824 704 is gratefully acknowledged. We thank BASF SE for the supply of aluminum fumarate and the group of Lena Schnabel at the Fraunhofer ISE and especially Ursula Wittstadt for measurements and further support.

■ ABBREVIATIONS

AHP = adsorption heat pump
COP = coefficient of performance
HX = heat-exchanger
MOF = metal−organic framework
TDC = thermally driven chiller
SCP = specific cooling power
VSCP = volume specific cooling power

■ REFERENCES

(1) Kuppler, R. J.; Timmons, D. J.; Fang, Q.-R.; Li, J.-R.; Makal, T. A.; Young, M. D.; Yuan, D.; Zhao, D.; Zhuang, W.; Zhou, H.-C. Potential applications of metal-organic frameworks. *Coord. Chem. Rev.* **2009**, *253*, 3042−3066.
(2) Suh, M. P.; Park, H. J.; Prasad, T. K.; Lim, D. W. Hydrogen storage in metal-organic frameworks. *Chem. Rev.* **2012**, *112*, 782−835.
(3) Murray, L. J.; Dincă, M.; Long, J. R. Hydrogen storage in metal-organic frameworks. *Chem. Soc. Rev.* **2009**, *38*, 1294−1314.
(4) Mason, J. A.; Veenstra, M.; Long, J. R. Evaluating metal−organic frameworks for natural gas storage. *Chem. Sci.* **2014**, *5*, 32.
(5) Alezi, D.; Belmabkhout, Y.; Suyetin, M.; Bhatt, P. M.; Weseliński, Ł. J.; Solovyeva, V.; Adil, K.; Spanopoulos, I.; Trikalitis, P. N.; Emwas, A.-H.; Eddaoudi, M. MOF Crystal Chemistry Paving the Way to Gas Storage Needs: Aluminum-Based soc-MOF for CH_4, O_2, and CO_2 Storage. *J. Am. Chem. Soc.* **2015**, *137*, 13308−13318.
(6) Li, Y.; Yang, R. T. Gas Adsorption and Storage in Metal−Organic Framework MOF-177. *Langmuir* **2007**, *23*, 12937−12944.
(7) Purewal, J.; Liu, D.; Sudik, A.; Veenstra, M.; Yang, J.; Maurer, S.; Müller, U.; Siegel, D. J. Improved Hydrogen Storage and Thermal Conductivity in High-Density MOF-5 Composites. *J. Phys. Chem. C* **2012**, *116*, 20199−20212.
(8) Zheng, B.; Yun, R.; Bai, J.; Lu, Z.; Du, L.; Li, Y. Expanded Porous MOF-505 Analogue Exhibiting Large Hydrogen Storage Capacity and Selective Carbon Dioxide Adsorption. *Inorg. Chem.* **2013**, *52*, 2823−2829.
(9) Hu, J.; Cai, H.; Ren, H.; Wei, Y.; Xu, Z.; Liu, H.; Hu, Y. Mixed-Matrix Membrane Hollow Fibers of $Cu_3(BTC)_2$ MOF and Polyimide for Gas Separation and Adsorption. *Ind. Eng. Chem. Res.* **2010**, *49*, 12605−12612.
(10) Huang, W.; Jiang, J.; Wu, D.; Xu, J.; Xue, B.; Kirillov, A. M. A Highly Stable Nanotubular MOF Rotator for Selective Adsorption of Benzene and Separation of Xylene Isomers. *Inorg. Chem.* **2015**, *54*, 10524−10526.
(11) Verma, P.; Xu, X.; Truhlar, D. G. Adsorption on Fe-MOF-74 for C1−C3 Hydrocarbon Separation. *J. Phys. Chem. C* **2013**, *117*, 12648−12660.
(12) Zhao, Z.; Ma, X.; Kasik, A.; Li, Z.; Lin, Y. S. Gas Separation Properties of Metal Organic Framework (MOF-5) Membranes. *Ind. Eng. Chem. Res.* **2013**, *52*, 1102−1108.
(13) Wisser, D.; Wisser, F. M.; Raschke, S.; Klein, N.; Leistner, M.; Grothe, J.; Brunner, E.; Kaskel, S. Biological Chitin-MOF Composites with Hierarchical Pore Systems for Air-Filtration Applications. *Angew. Chem., Int. Ed.* **2015**, *54*, 12588−12591.
(14) Cychosz, K. A.; Ahmad, R.; Matzger, A. J. Liquid phase separations by crystalline microporous coordination polymers. *Chem. Sci.* **2010**, *1*, 293−302.
(15) Han, S.; Wei, Y.; Valente, C.; Lagzi, I.; Gassensmith, J. J.; Coskun, A.; Stoddart, J. F.; Grzybowski, B. A. Chromatography in a Single Metal−Organic Framework (MOF) Crystal. *J. Am. Chem. Soc.* **2010**, *132*, 16358−16361.
(16) Moreira, M. A.; Santos, J. C.; Ferreira; Alexandre, F. P.; Loureiro, J. M.; Ragon, F.; Horcajada, P.; Shim, K.-E.; Hwang, Y.-K.; Lee, U.-H.; Chang, J.-S.; Serre, C.; Rodrigues, A. E. Reverse Shape Selectivity in the Liquid-Phase Adsorption of Xylene Isomers in Zirconium Terephthalate MOF UiO-66. *Langmuir* **2012**, *28*, 5715−5723.
(17) Wang, L.; Li, Y.-A.; Yang, F.; Liu, Q.-K.; Ma, J.-P.; Dong, Y.-B. Cd(II)-MOF: Adsorption, Separation, and Guest-Dependent Luminescence for Monohalobenzenes. *Inorg. Chem.* **2014**, *53*, 9087−9094.
(18) Herbst, A.; Khutia, A.; Janiak, C. Brønsted Instead of Lewis Acidity in Functionalized MIL-101Cr MOFs for Efficient Heterogeneous (nano-MOF) Catalysis in the Condensation Reaction of Aldehydes with Alcohols. *Inorg. Chem.* **2014**, *53*, 7319−7333.
(19) Corma, A.; Garcia, H.; Llabres i Xamena, F. X. Engineering metal organic frameworks for heterogeneous catalysis. *Chem. Rev.* **2010**, *110*, 4606−4655.
(20) Dang, D.; Wu, P.; He, C.; Xie, Z.; Duan, C. Homochiral Metal−Organic Frameworks for Heterogeneous Asymmetric Catalysis. *J. Am. Chem. Soc.* **2010**, *132*, 14321−14323.
(21) Gole, B.; Sanyal, U.; Banerjee, R.; Mukherjee, P. S. High Loading of Pd Nanoparticles by Interior Functionalization of MOFs for Heterogeneous Catalysis. *Inorg. Chem.* **2016**, *55*, 2345−2354.
(22) Müller, M.; Hermes, S.; Kähler, K.; van den Berg, M. W. E.; Muhler, M.; Fischer, R. A. Loading of MOF-5 with Cu and ZnO Nanoparticles by Gas-Phase Infiltration with Organometallic Precursors: Properties of Cu/ZnO@MOF-5 as Catalyst for Methanol Synthesis. *Chem. Mater.* **2008**, *20*, 4576−4587.
(23) Horcajada, P.; Gref, R.; Baati, T.; Allan, P. K.; Maurin, G.; Couvreur, P.; Férey, G.; Morris, R. E.; Serre, C. Metal-organic frameworks in biomedicine. *Chem. Rev.* **2012**, *112*, 1232−1268.
(24) Bhardwaj, S. K.; Bhardwaj, N.; Mohanta, G. C.; Kumar, P.; Sharma, A. L.; Kim, K.-H.; Deep, A. Immunosensing of Atrazine with Antibody-Functionalized Cu-MOF Conducting Thin Films. *ACS Appl. Mater. Interfaces* **2015**, *7*, 26124−26130.
(25) Cui, L.; Wu, J.; Li, J.; Ju, H. Electrochemical Sensor for Lead Cation Sensitized with a DNA Functionalized Porphyrinic Metal−Organic Framework. *Anal. Chem.* **2015**, *87*, 10635−10641.
(26) Drobek, M.; Kim, J.-H.; Bechelany, M.; Vallicari, C.; Julbe, A.; Kim, S. S. MOF-Based Membrane Encapsulated ZnO Nanowires for Enhanced Gas Sensor Selectivity. *ACS Appl. Mater. Interfaces* **2016**, *8*, 8323−8328.
(27) Ranft, A.; Niekiel, F.; Pavlichenko, I.; Stock, N.; Lotsch, B. V. Tandem MOF-Based Photonic Crystals for Enhanced Analyte-Specific Optical Detection. *Chem. Mater.* **2015**, *27*, 1961−1970.
(28) Schoenecker, P. M.; Carson, C. G.; Jasuja, H.; Flemming; Christine, J. J.; Walton, K. S. Effect of Water Adsorption on Retention of Structure and Surface Area of Metal−Organic Frameworks. *Ind. Eng. Chem. Res.* **2012**, *51*, 6513−6519.
(29) Jasuja, H.; Huang, Y. G.; Walton, K. S. Adjusting the stability of metal-organic frameworks under humid conditions by ligand functionalization. *Langmuir* **2012**, *28*, 16874−16880.
(30) Burtch, N. C.; Jasuja, H.; Walton, K. S. Water stability and adsorption in metal-organic frameworks. *Chem. Rev.* **2014**, *114*, 10575−10612.
(31) Fröhlich, D.; Henninger, S. K.; Janiak, C. Multicycle water vapour stability of microporous breathing MOF aluminium isophthalate CAU-10-H. *Dalton Trans.* **2014**, *43*, 15300−15304.
(32) Henninger, S. K.; Jeremias, F.; Kummer, H.; Janiak, C. MOFs for Use in Adsorption Heat Pump Processes. *Eur. J. Inorg. Chem.* **2012**, 2625−2634.

DOI: 10.1021/acs.iecr.7b00106
Ind. Eng. Chem. Res. 2017, 56, 8393−8398

(33) Henninger, S. K.; Jeremias, F.; Kummer, H.; Schossig, P.; Henning, H.-M. Novel Sorption Materials for Solar Heating and Cooling. *Energy Procedia* **2012**, *30*, 279−288.
(34) Jeremias, F.; Fröhlich, D.; Janiak, C.; Henninger, S. K. Advancement of sorption-based heat transformation by a metal coating of highly-stable, hydrophilic aluminium fumarate MOF. *RSC Adv.* **2014**, *4*, 24073−24082.
(35) Jeremias, F.; Fröhlich, D.; Janiak, C.; Henninger, S. K. Water and methanol adsorption on MOFs for cycling heat transformation processes. *New J. Chem.* **2014**, *38*, 1846−1852.
(36) Jeremias, F.; Khutia, A.; Henninger, S. K.; Janiak, C. MIL-100(Al, Fe) as water adsorbents for heat transformation purposes—a promising application. *J. Mater. Chem.* **2012**, *22*, 10148−10151.
(37) Jeremias, F.; Lozan, V.; Henninger, S.; Janiak, C. Programming MOFs for water sorption: Amino-functionalized MIL-125 and UiO-66 for heat transformation and heat storage applications. *Dalton Trans.* **2013**, *42*, 15967−15973.
(38) Jasuja, H.; Zang, J.; Sholl, D. S.; Walton, K. S. Rational Tuning of Water Vapor and CO_2Adsorption in Highly Stable Zr-Based MOFs. *J. Phys. Chem. C* **2012**, *116*, 23526−23532.
(39) de Lange, M. F.; Verouden, K. J. F. M.; Vlugt, T. J. H.; Gascon, J.; Kapteijn, F. Adsorption-Driven Heat Pumps: The Potential of Metal−Organic Frameworks. *Chem. Rev.* **2015**, *115*, 12205.
(40) Aristov, Y. I. Novel Materials for Adsorptive Heat Pumping and Storage: Screening and Nanotailoring of Sorption Properties. *J. Chem. Eng. Jpn.* **2007**, *40*, 1242−1251.
(41) de Lange, M. F.; Ottevanger, C. P.; Wiegman, M.; Vlugt, T. J. H.; Gascon, J.; Kapteijn, F. Crystals for sustainability − structuring Al-based MOFs for the allocation of heat and cold. *CrystEngComm* **2015**, *17*, 281−285.
(42) Gordeeva, L. G.; Solovyeva, M. V.; Aristov, Y. I. NH2-MIL-125 as a promising material for adsorptive heat transformation and storage. *Energy* **2016**, *100*, 18−24.
(43) Alvarez, E.; Guillou, N.; Martineau, C.; Bueken, B.; Van de Voorde, B.; Le Guillouzer, C.; Fabry, P.; Nouar, F.; Taulelle, F.; de Vos, D.; Chang, J. S.; Cho, K. H.; Ramsahye, N.; Devic, T.; Daturi, M.; Maurin, G.; Serre, C. The Structure of the Aluminum Fumarate Metal-Organic Framework A520. *Angew. Chem., Int. Ed.* **2015**, *54*, 3664.
(44) Gaab, M.; Trukhan, N.; Maurer, S.; Gummaraju, R.; Müller, U. The progression of Al-based metal-organic frameworks − From academic research to industrial production and applications. *Microporous Mesoporous Mater.* **2012**, *157*, 131−136.
(45) Henninger, S. K.; Schmidt, F. P.; Henning, H.-M. Characterisation and improvement of sorption materials with molecular modeling for the use in heat transformation applications. *Adsorption* **2011**, *17*, 833−843.
(46) Aristov, Y. I. Challenging offers of material science for adsorption heat transformation: A review. *Appl. Therm. Eng.* **2013**, *50*, 1610−1618.
(47) Freni, A.; Maggio, G.; Sapienza, A.; Frazzica, A.; Restuccia, G.; Vasta, S. Comparative analysis of promising adsorbent/adsorbate pairs for adsorptive heat pumping, air conditioning and refrigeration. *Appl. Therm. Eng.* **2016**, *104*, 85−95.
(48) Aristov, Y. I. Adsorptive transformation and storage of renewable heat: Review of current trends in adsorption dynamics. *Renewable Energy* **2016**, *110*, 105.
(49) Chakraborty, A.; Saha, B. B.; Aristov, Y. I. Dynamic behaviors of adsorption chiller: Effects of the silica gel grain size and layers. *Energy* **2014**, *78*, 304−312.
(50) Wittstadt, U.; Füldner, G.; Andersen, O.; Herrmann, R.; Schmidt, F. A New Adsorbent Composite Material Based on Metal Fiber Technology and Its Application in Adsorption Heat Exchangers. *Energies* **2015**, *8*, 8431−8446.
(51) Freni, A.; Dawoud, B.; Bonaccorsi, L.; Chmielewski, S.; Frazzica, A.; Calabrese, L.; Restuccia, G. *Characterization of Zeolite-Based Coatings for Adsorption Heat Pumps*; SpringerBriefs in Applied Sciences and Technology; Springer, 2015.
(52) Dawoud, B. Water vapor adsorption kinetics on small and full scale zeolite coated adsorbers; A comparison. *Appl. Therm. Eng.* **2013**, *50*, 1645−1651.
(53) Tu, Y. D.; Wang, R. Z.; Ge, T. S.; Zheng, X. Comfortable, high-efficiency heat pump with desiccant-coated, water-sorbing heat exchangers. *Sci. Rep.* **2017**, *7*, 40437.
(54) Jiang, Y.; Ge, T. S.; Wang, R. Z.; Hu, L. M. Experimental investigation and analysis of composite silica-gel coated fin-tube heat exchangers. *Int. J. Refrig.* **2015**, *51*, 169−179.
(55) Zhao, Y.; Ge, T. S.; Dai, Y. J.; Wang, R. Z. Experimental investigation on a desiccant dehumidification unit using fin-tube heat exchanger with silica gel coating. *Appl. Therm. Eng.* **2014**, *63*, 52−58.
(56) Frazzica, A.; Füldner, G.; Sapienza, A.; Freni, A.; Schnabel, L. Experimental and theoretical analysis of the kinetic performance of an adsorbent coating composition for use in adsorption chillers and heat pumps. *Appl. Therm. Eng.* **2014**, *73*, 1022−1031.
(57) Kummer, H.; Füldner, G.; Henninger, S. K. Versatile siloxane based adsorbent coatings for fast water adsorption processes in thermally driven chillers and heat pumps. *Appl. Therm. Eng.* **2015**, *85*, 1.
(58) Bendix, P. B.; Henninger, S. K.; Henning, H.-M. Temperature and mechanical stabilities and changes in porosity of silicone binder based zeolite coatings. *Ind. Eng. Chem. Res.* **2016**, *55*, 4942.
(59) Jeremias, F.; Henninger, S. K.; Janiak, C. High performance metal-organic-framework coatings obtained via thermal gradient synthesis. *Chem. Commun.* **2012**, *48*, 9708−9710.
(60) Kummer, H.; Baumgartner, M.; Hügenell, P.; Fröhlich, D.; Henninger, S. K.; Gläser, R. Thermally driven refrigeration by methanol adsorption on coatings of HKUST-1 and MIL-101(Cr). *Appl. Therm. Eng.* **2016**, *117*, 689.
(61) Fröhlich, D.; Pantatosaki, E.; Kolokathis, P. D.; Markey, K.; Reinsch, H.; Baumgartner, M.; van der Veen, M. A.; de Vos, D. E.; Stock, N.; Papadopoulos, G. K.; Henninger, S. K.; Janiak, C. adsorption behaviour of CAU-10-H: A thorough investigation of its structure−property relationships. *J. Mater. Chem. A* **2016**, *4*, 11859−11869.
(62) Solovyeva, M. V.; Aristov, Y. I.; Gordeeva, L. G. NH2-MIL-125 as promising adsorbent for adsorptive cooling: Water adsorption dynamics. *Appl. Therm. Eng.* **2017**, *116*, 541−548.

DOI: 10.1021/acs.iecr.7b00106
Ind. Eng. Chem. Res. 2017, 56, 8393−8398